Biological
Cybernetics

Analysis of mechanical impedance in human arm movements using a virtual tennis system

Toshio Tsuji, Yusaku Takeda, Yoshiyuki Tanaka

Department of Artificial Complex Systems Engineering, Hiroshima University, 4-1 Kagamiyama 1-chome, Higashi-Hiroshima, Hiroshima, Japan

Abstract. The dynamic characteristics of human upper extremities are usually expressed by mechanical impedance. Although many studies have discussed human impedance characteristics, there are no reports on control abilities of task-related impedance in skilled human hand movements.

This paper proposes a virtual sports system using a virtual reality technique to examine human movements. The differences in movements between skilled and unskilled subjects are investigated through a series of experiments. Then, the human impedance of a skilled player is estimated and analyzed in the preliminary phase of motion.

1 Introduction

Humans perform a variety of skillful movements by adjusting dynamic characteristics of their musculoskeletal system in motion. For example, a professional tennis player can serve an extraordinarily fast ball through an arc-shaped movement of his arm. The player has not only strong muscle power but also the ability to control his arm dynamics. In general, such dynamics of a hand–arm system have often been discussed in relation to the operational task space by using mechanical impedance parameters, i.e., hand stiffness, hand viscosity, and hand inertia.

Many experimental studies on human arm impedance have been reported. For example, Mussa-Ivaldi et al. (1985) pioneered the measurement of human hand impedance and examined hand stiffness in a stable arm posture. It was reported that hand stiffness depends greatly on the arm posture and that humans could change at will the magnitude of stiffness but not its direction. Also, Dolan et al. (1993) and Tsuji et al. (1994, 1995) investigated not only hand stiffness but also viscosity and inertia and verified a qualitative analogy between hand stiffness and viscosity. Tsuji et al. (1996) found that hand

Correspondence to: T. Tsuji
(e-mail: tsuji@bsys.hiroshima-u.ac.jp,
Tel.: +81-824-247677, Fax: +81-824-227030)

viscoelastic characteristics change in proportion to the muscle contraction level. Gomi and Kawato (1997) then examined hand impedance in reaching movements and demonstrated that hand stiffness in motion changes activity more than once in a stable arm posture.

Human impedance has also been used for kinesitherapy in rehabilitation (Hogan et al. 1993; Krebs et al. 1996; Tsuji et al. 1999). Hogan et al. (1993) and Krebs et al. (1996), for example, developed a new training system using the impedance-controlled robot with parallel mechanism. However, they did not train the trainee's ability to control impedance itself. Tsuji et al. (1999) proposed the impedance training to improve a trainee's ability to regulate voluntary impedance. The trainee is asked to adjust his hand impedance in such a way that the hand impedance, which can be measured during the training online, agrees with the target impedance. They verified that the ability to regulate impedance can be improved effectively by a prototype training system based on the impedance training method. They also described the primary factors for the effective regulation of impedance parameters, i.e., muscle contraction level for stiffness, motion direction for viscosity, and arm posture for inertia. However, the developed training system can be applied only to static motions with a maintained posture, not to skill training associated with dynamic motion.

Sports exercises are good potential examples of the impedance training of dynamic movements. There are difficulties, however, in measuring force and positional information in human motion. Also, in the impedance training method, it is necessary to apply an external disturbance to the trainee's hand movements during dynamic movements in order to estimate the human hand impedance. Such operations may be extremely difficult to conduct while the sports exercises are taking place. Although some reports have attempted to estimate human impedance parameters in dynamic motion from EMG signals (Tsuji et al. 1996; Tsuji and Kaneko 1996; Osu and Gomi 1999), hand impedance cannot be expected to be measured accurately in motion because human impedance is influenced significantly by the conditions of the musculoskeletal system depending on the contraction intensity,

arrangement of various muscles, and sensitivity of the spinal reflex.

The present paper develops a virtual sports system as a first step toward realizing impedance training in dynamic motion by utilizing a virtual reality technique and an impedance-controlled robot. It should be noted that the main purpose of this paper is not to realize "real sports" in the virtual reality environment. The most important feature of the proposed virtual sports system is that the system makes it possible to apply an external disturbance to a trainee's motion. The measurement of human hand impedance in a virtual sport allows us to analyze muscular activities that play an important role in acquiring task-related hand impedance characteristics that should be useful for sports training and rehabilitation Tsuji et al. (2001).

2 Virtual tennis system

2.1 Experimental equipment

Figure 1 depicts a prototype system for virtual sports training in which a trainee can play virtual tennis. The trainee is required to hit a computer-controlled virtual ball by operating a handle attached to a robot instead of hitting an actual tennis ball, while the robot displays interaction force to the trainee in hitting the ball. The robot in the training system is constructed with a linear motor table (Nippon Thompson Co., Ltd., Tokyo; maximum driving
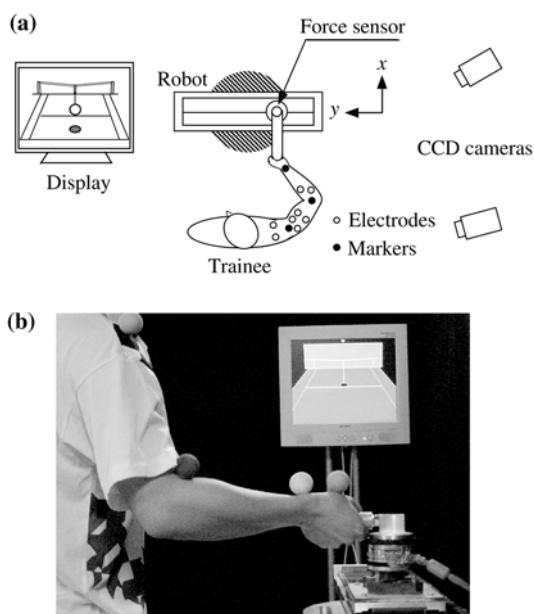

Fig. 1a,b. Virtual tennis system. **a** System configuration. **b** A trainee playing virtual tennis. The trainee is requested to hit a computer-controlled virtual ball instead of an actual tennis ball by operating a handle attached to a robot while the robot displays interaction force to the trainee in hitting the ball. To investigate a mechanism of human impedance regulation, surface EMG signals are measured from eight muscles of the trainee's arm. The stereo video camera system with two CCD cameras can measure the arm posture of a trainee by detecting color markers attached to the trainee

force 10 kgf; encoder resolution 2 μm) that is impedance-controlled so that the virtual interaction force between the virtual ball and the racket handle can be displayed to the trainee. A six-axis force sensor (B.L. Autotech Co., Ltd., Kobe, Japan; resolution: translational force on the x- and y-axes 5×10^{-3} N, on the z-axis 15×10^{-2} N Ctorque 3×10^{-3} Nm) is attached at the base of the handle to measure the operating hand force of the trainee. The trainee can play virtual tennis on the basis of the visual information provided on the display. A human can change his hand impedance by adjusting the muscle contraction level as well as arm posture Tsuji et al. (1996). To investigate a mechanism of human impedance regulation, surface EMG signals in the training are measured from the flexor (flexor carpi radialis, FCR) and the extensor (extensor ulnaris, ECU) in the wrist joint, the flexor (biceps brachii, BB) and extensor (triceps brachii, TB) in the elbow joint, and the flexors (pectoralis major, PM; deltoideus anterior, DA) and extensors (teres major, TM; deltoideus posterior, DP) in the shoulder joint. The sampling rate for hand movements and EMG signals was set at 1 kHz in the experiments. Also, the stereo video camera system with two CCD cameras (Quick MAG: Oh-yoh Keisoku Kenkyusho, sampling rate: 60 Hz) are utilized to observe the arm posture of a trainee by detecting color markers attached to him.

2.2 Model of virtual tennis

Figure 2a shows a model of virtual tennis in which a trainee hits a virtual ball so as to make the ball bounce off a wall. The virtual ball is represented by a viscoelastic model on the assumption that the mass is concentrated at the center of the ball as shown in Fig. 2b, where the model parameters are determined with consideration of the racket strings. The racket is regarded as a flat board parallel to the x–z plane with an infinite length in both the x- and z-axes and has only one degree of freedom along the y-axis. Also, the racket has an inclination θ from the y-axis. The virtual ball moves with two degrees of freedom on the y–z plane.
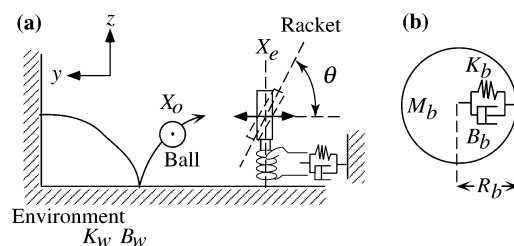
Fig. 2a,b. Model of virtual tennis. **a** A trainee hits a virtual ball so as to make the ball bounce off a wall, where X_o [$=(0, X_{oy}, X_{oz})$] denotes the center position of the ball, X_e is the racket position, and θ is the inclination of the racket from the y-axis. **b** The virtual ball is represented by a viscoelastic model under the assumption that the mass is concentrated at the center of the ball, where the model parameters are determined with a consideration of the racket strings. M_b is the mass of the ball. The viscoelastic properties of the ball, K_b and B_b, are defined together with the corresponding properties of a racket string by (7) and (8)

Then, the motion equation of the racket can be written as follows:

$$M_r \ddot{X}_{ey} + B_r \dot{X}_{ey} = F_y + F_e \,, \tag{1}$$

where F_y denotes the interaction force applied from the virtual ball to the racket along the y-axis, F_e is the operating hand force, X_{ey} is the racket position on the y-axis, and M_r and B_r are the target inertia and target viscosity of the robot, respectively. The trainee can enjoy a realistic feel of the racket handle characterized by M_r and B_r and perceive a virtual interaction force upon hitting the virtual ball.

Dynamic behaviors of the virtual ball can be given by the following equations:

$$M_b \ddot{X}_{oy} = -F_y + F_{wy} \,, \tag{2}$$
$$M_b \ddot{X}_{oz} = -F_z + F_{wz} - M_b g \,, \tag{3}$$

where $X_o [= (0, X_{oy}, X_{oz})^T]$ denotes the center position of the ball; M_b is the mass of the ball; F_y and F_z are interaction forces in the y- and z-axes upon impact, respectively; F_{wy} and F_{wz} are the reaction forces as the ball rebounds off the wall and the floor, respectively; and g represents the gravitational acceleration. F_y and F_z are calculated as follows:

$$F_y = \begin{cases} B_b(dX_{by}) d\dot{X}_{by} + K_b(dX_{by}) dX_{by} & (|X_{ry}| \le R_b) \\ 0 & (|X_{ry}| > R_b) \,, \end{cases} \tag{4}$$
$$F_z = F_y \tan\theta \,, \tag{5}$$
$$dX_{by} = X_{ry} - R_b, \tag{6}$$

where $X_{ry} [= X_{oy} - X_{ey}]$ represents the relative position of the ball and the racket, θ is the inclination of the racket from the y-axis, and dX_{by} is the displacement of the ball due to impact. Note that the reaction force of the ball can be generated in the z direction as well as the y direction. The viscoelastic properties of the ball, $K_b(dX_{by})$ and $B_b(dX_{by})$, are defined together with those of a racket string by

$$K_b(dX_{by}) = 318.5 + 11452.8|dX_{by}| \,, \tag{7}$$
$$B_b(dX_{by}) = 2\zeta_b \sqrt{M_b K_b(dX_{by})} \,, \tag{8}$$

where ζ_b denotes the damping coefficient. Each parameter was designed by trial and error on the basis of the reference study by Kawazoe (1992). F_{wy} and F_{wz} in (2) and (3) are expressed with a viscoelastic model as

$$F_{wi} = \begin{cases} B_w(dX_{wi}) d\dot{X}_{wi} + K_w(dX_{wi}) dX_{wi} & (|X_{si}| \le R_b) \\ 0 & (|X_{si}| > R_b) \,, \end{cases} \tag{9}$$
$$dX_{wi} = X_{si} - R_b n_i \,, \tag{10}$$
$$n_i = \begin{cases} \dfrac{X_{si}}{|X_{si}|} & (X_{si} \ne 0) \,, \\ 0 & (X_{si} = 0) \,, \end{cases} \tag{11}$$

where $i \in \{y, z\}$, $X_{si} (= X_{oi} - X_{wi})$ represents the relative position of the ball and the environment, and X_{wy} and X_{wz} are the positions of the wall and the floor, respectively. $K_w(dX_{wi})$ and $B_w(dX_{wi})$ are the stiffness and the
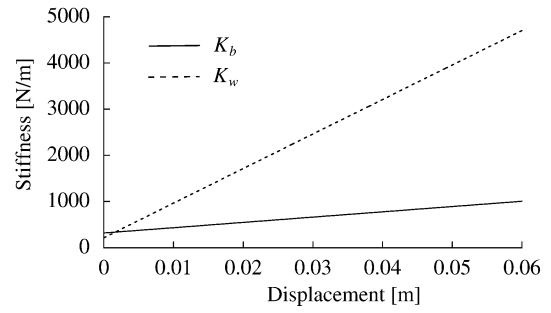
Fig. 3. Resultant stiffness of the ball-and-strings system (K_b) and the ball-and-environment system (K_w). The nonconstant stiffness characteristics enable us to generate a nonlinear interaction force so that the trainee can have a realistic feeling of hitting a real ball

viscosity of the ball upon impact with the environment expressed by

$$K_w(dX_{wi}) = 214.6 + 75068|dX_{wi}| \,, \tag{12}$$
$$B_w(dX_{wi}) = 2\zeta_w \sqrt{M_b K_w(dX_{wi})} \,, \tag{13}$$

where ζ_w is the damping coefficient.

Figure 3 illustrates the relation between the stiffness and the displacement of the virtual ball where the solid line represents $K_b(dX_{by})$ and the broken line $K_w(dX_{wi})$. The nonconstant stiffness of (12) and (13) enables us to generate a nonlinear interaction force so that the trainee can have a realistic feeling of hitting a real ball. Note that the damping characteristics of the ball can be regulated by ζ_b and ζ_w.

2.3 Impedance control

Figure 4a represents a block diagram of the developed human-robot system for virtual tennis training, and Fig. 4b explains the impedance control part. The robot is impedance controlled by a control input F_{act} Hogan (1985), while the dynamic behavior of the racket handle follows (1).

The dynamics of the robot under the impedance control can be expressed by
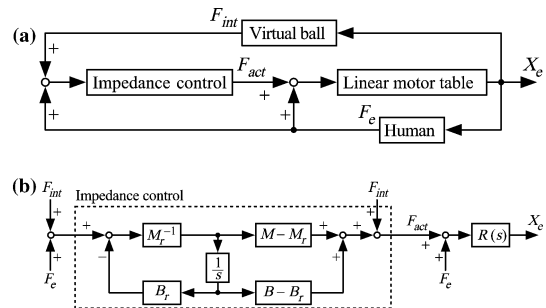
Fig. 4a,b. Impedance control system for virtual tennis. **a** Block diagram of the control system of the developed virtual tennis system. **b** Impedance control part. The robot is impedance controlled by a control input F_{act} Hogan (1985), while the dynamic behavior of the racket handle follows (1). The dynamics of the robot under the impedance control can be expressed by (14), where M and B denote, respectively, the desired inertia and the desired viscous friction of the robot
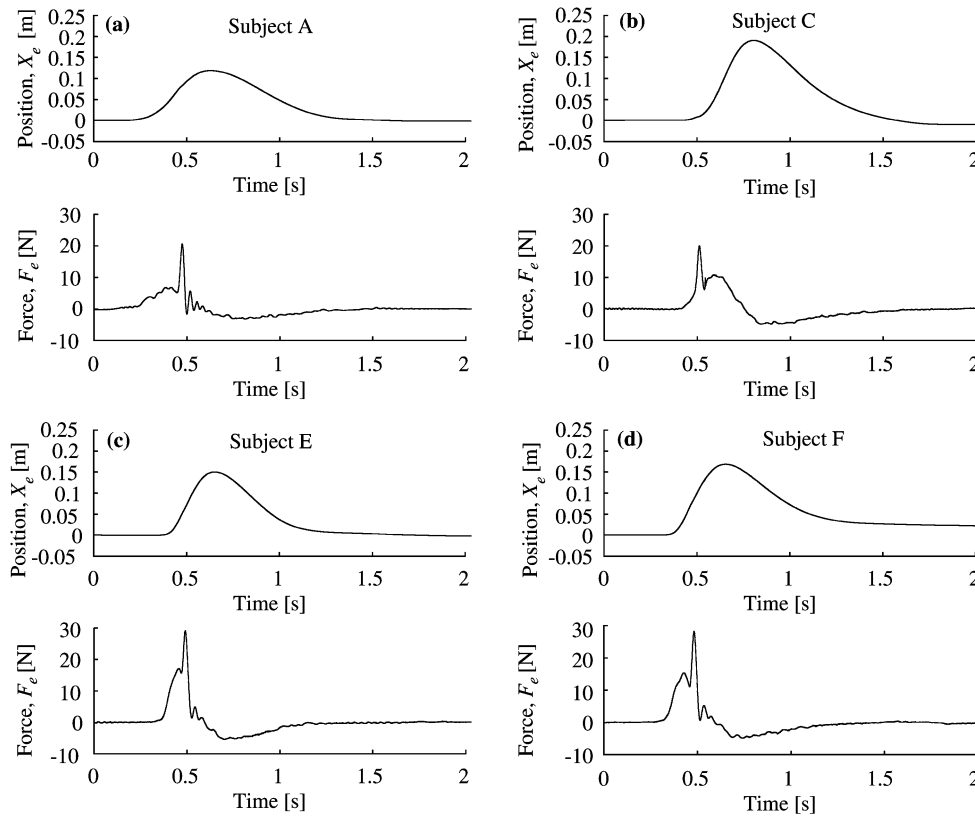
Fig. 5a–d. Examples of time histories of hand position and hand force by subjects A, C, E, and F (**a–d**). **a** A successful trial by the well-trained subjects. **b–d** Failed trials by the untrained subjects

$$R(s) = \frac{1}{Ms^2 + Bs}, \tag{14}$$

where M and B denote, respectively, the desired inertia and the desired viscous friction of the robot. In this paper, these robot motion control parameters are set at $M = 4.7$ kg and $B = 47.0$ Ns/m, and the target impedance is set at $M_r = 0.9$ kg, $B_r = 0$ Ns/m, and $K_r = 0$ N/s.

3 Analysis of human movements in virtual tennis

3.1 Experiments

Human movements in virtual tennis were measured for two well-trained subjects (A and B), who had gone through skill-acquisition training for virtual tennis in advance, and four untrained subjects (C, D, E, and F). Based on preliminary experiments, the inclination of the racket was set at $\theta = 0.349$ rad, the distance between the racket and the wall was 2 m, the initial position of the ball $X_o(0) = (0.0, 1.0, 0.5)$ m, the initial speed of the ball $\dot{X}_o(0) = (0.0, -2.0, 3.0)$ m/s, the mass of the ball $M_b = 0.1$ kg, and the radius of the ball $R_b = 0.06$ m. The origin of the x- and y-axes was settled at the initial position of the racket, and the virtual ground coincided with the x–y plane ($z = 0$). The damping coefficients of the virtual ball were set at $\zeta_b = 0.06$, $\zeta_w = 0.15$ on the basis of the experimental data for the rebounding behavior of a real ball, in which the ball was released from a height of 1 m under free-fall.

Each subject in the training experiments was asked to strike the ball, thrown from the front, just one time so as to hit a specified round target with a radius of 0.1 m on the wall. The release time of the virtual ball was indicated on the display 3 s in advance. The extent of the subject's skill was evaluated by the success rate of hitting the target.

3.2 Experimental results

Figure 5 represents examples of the time histories of hand position and hand force by the subjects, where Fig. 5a shows a successful trial by the well-trained subjects while the others represent failed trials by the untrained subjects. Table 1 shows the rates of successful trials for each subject.

It can be seen from the time profiles of hand position that the subjects hit the ball by thrusting the racket handle forward without taking a backward swing. The subjects attempted to swing the racket in hopes of hitting the ball with appropriate timing. There exist differences in the hand force profiles between the well-trained subjects and the untrained subjects. The impact force appears just around the peak of the hand force profile in Fig. 5a. This means that the well-trained subjects could hit the ball with maximum hand force. By contrast, in the failed trials by the untrained subjects (Fig. 5b–d), the impact force is

Table 1. Rates of successful trials (subjects A–F)

Subject	A	B	C	D	E	F
Successful rate	91.2	85.7	56.5	59.6	28.8	30.0
No. of trials	107	121	105	118	96	109
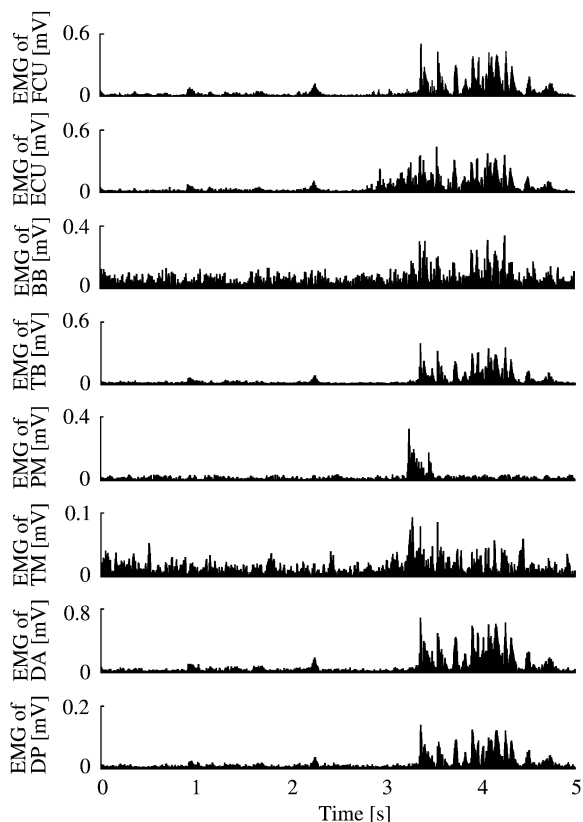
Fig. 6. Example of the measured EMG signals (subject A). The EMG signal was measured for 5 s beginning 3 s before the ball was thrown. The subject prepared for hitting the ball by contracting each muscle in the preliminary phase

observed before or after the peak of the hand force profile, and three types were found as follows:

1. The subject in Fig. 5b hit the ball too early; he maximized hand force before hitting the ball.
2. The untrained subject in Fig. 5c generated the maximum force at the moment of impact, but it was much larger than that of a well-trained subject.
3. The untrained subject in Fig. 5d hit the ball too late; he generated hand force in a flurry after impact with the ball.

We see that a subject playing virtual tennis must generate and control his hand force F_e according to the ball motion so as to hit the target.

Figure 6 illustrates an example of the full-wave rectified EMG signals of subject A during virtual tennis in which the EMG signal was measured for 5 s beginning 3 s before the ball was thrown. The subject prepared for hitting the ball by contracting each muscle in the preliminary phase. It must be noted that the subject could regulate his hand impedance in operating the racket handle by changing the muscle contraction levels of both flexor and extensor in his wrist joint (Tsuji et al. 1996; Gomi and Kawato 1996).

Figure 7 shows an example of the arm postures of subject B while playing virtual tennis. Note that the subject swung his arm by actively changing the elbow and the shoulder joint angles. Thus, the developed virtual sports
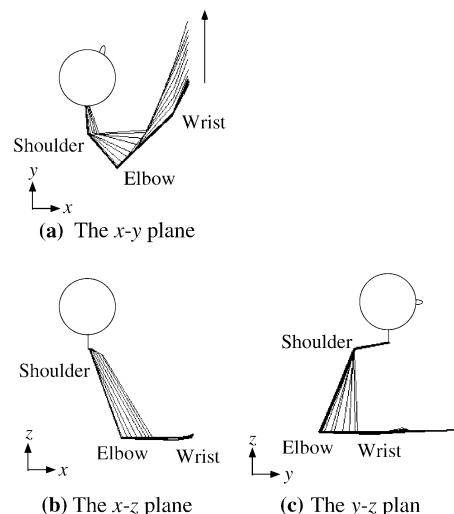

Fig. 7a–c. Example of arm postures while playing virtual tennis (subject B). The subject swung his arm by actively changing the elbow and shoulder joint angles

training system can measure dynamic movements of a trainee playing virtual sports such as hand movements, surface EMG signals, and arm postures.

3.3 Process of skill acquisition

The experimental results with the untrained subjects (subjects C, D, E, and F) demonstrate that subjects can be classified into two groups differentiated by the skill acquisition process. Subjects C and D progressed by hitting the target after repeated trials, while subjects E and F could not succeed in the end. This subsection discusses the change of motions of subjects C and D.

Figure 8 shows examples of the time profiles of hand position and hand force by subject C before and after skill
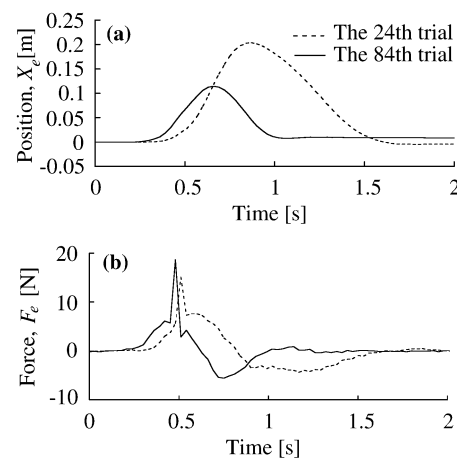
Fig. 8a–b. Examples of the time profiles of hand position and hand force by subject C before and after skill acquisition (in the 24th and 84th trials). The *broken line* in the figure represents the experimental result before skill acquisition and the *solid line* the result after skill acquisition
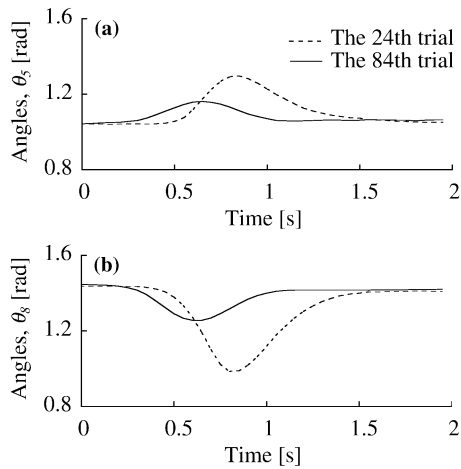
Fig. 9a,b. Time histories of the horizontal flexion-extension angle of the shoulder joint θ_5 and the angle of the elbow joint θ_8 during virtual tennis
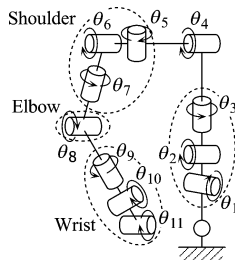
Fig. 10. Link model of a subject. The joint numbers in Fig. 9 are defined with a rigid link model of the right side of the upper half of the human body

acquisition (in the 24th and 84th trials). The broken line in the figure represents the experimental result before skill acquisition and the solid line the result after skill acquisition. Note that the skilled subject applies greater force to the racket from the beginning of the motion to swing the racket efficiently. These movements coincided with his joint motions in virtual tennis. Figure 9 shows time histories of the horizontal flexion-extension angle of the shoulder joint θ_5 and the angle of the elbow joint θ_8 during virtual tennis, where the joint numbers are defined with a rigid link model of the right side of the upper half of the human body depicted in Fig. 10. The broken line in Fig. 9 represents the result before skill acquisition and the solid line the result after skill acquisition. The skilled subject reduced wasteful joint motions for the target task and moved his arm efficiently.

The skill-acquiring course of an unskilled player can also be observed from his EMG signals in training experiments. Figure 11 depicts the full-wave rectified EMG signals before and after skill acquisition. Note that the subject discharges more EMG signals in preparation for movements and increases the muscle contraction level of both the flexor (FCU) and extensor (ECU) in the wrist joint after skill acquisition. This indicates that the skilled subject stiffens his wrist joint by regulating its impedance. The unskilled player makes progress in adapting his arm motion and impedance properties according to the target task through repeated practice.
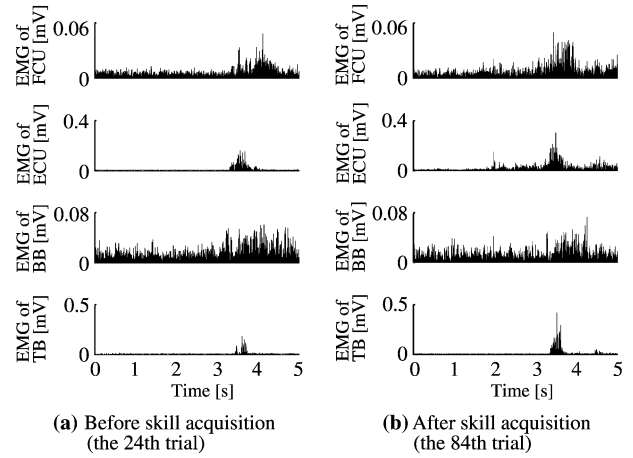

Fig. 11a,b. Example of the full-wave rectified EMG signals before and after skill acquisition (subject C)

4 Change of hand impedance depending on the environment

A set of experimental results of the EMG signals, as described in 3.2, suggests that humans regulate hand impedance not suddenly but gradually in preparation for motion. It is supposed that the impedance regulation is performed successfully in the motion of a well-trained subject. This section, then, investigates human hand impedance in the preparation phase to reveal how humans regulate hand impedance according to experimental conditions.

4.1 Impedance measurement

Let us consider a situation where a trainee is playing virtual tennis by operating the racket handle attached to the robot. When the subject's hand is displaced in the y direction from its equilibrium by a small disturbance with short
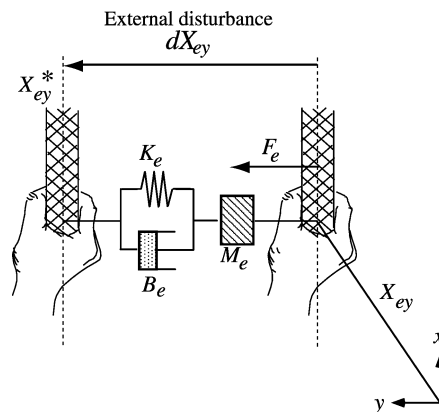
Fig. 12. Schematic description of hand impedance. While the subject maintains current hand position, an external disturbance to the hand is applied by a robot. Time changes of the hand displacements and forces caused by the disturbance are measured for estimating the hand impedance using a second-order linear model

duration as shown in Fig. 12, the dynamic properties of the hand can be approximated with mechanical impedance parameters as

$$M_e \mathrm{d}\ddot{X}_{ey}(t) + B_e \mathrm{d}\dot{X}_{ey}(t) + K_e dX_{ey}(t) = -F_e(t), \qquad (15)$$

where M_e, B_e, and K_e represent the hand inertia, viscosity, and stiffness, respectively, and $\mathrm{d}X_{ey}\ (= X^*_{ey}(t) - X_{ey}(t))$ denotes the distance between the hand position $X_{ey}(t)$ and the virtual trajectory $X^*_{ey}(t)$. $F_e(t)$ is the hand force corresponding to the external disturbance to the handle. The impedance parameters might be estimated by means of the least-squares method with the measured hand motion: $X_{ey}(t)$, $X^*_{ey}(t)$, and $F_e(t)$ (Tsuji et al. 1994, 1995). However, the virtual trajectory $X^*_{ey}(t)$ in dynamic motion is not measurable and may vary with a trainee's hand movements.

The unknown parameters M_e, B_e, K_e, and $X^*_{ey}(t)$ cannot be uniquely determined since the measurable parameters are only $X_{ey}(t)$, $\dot{X}_{ey}(t)$, $\ddot{X}_{ey}(t)$, and $F_e(t)$. Moreover, hand impedance should be regarded as a time-varying element because impedance parameters vary according to arm posture and muscle contraction level (Gomi and Kawato 1996). Consequently, it is very difficult to estimate the hand impedance in dynamic motion.

On the other hand, humans seem to regulate their impedance properties before motion, as suggested in Sect. 3.2. A player of virtual tennis should adjust his hand impedance just before hitting the ball according to the velocity and physical properties of the ball; otherwise, it would be too late to prepare for a hitting action. Thus, this paper focuses on hand impedance in the preparation phase, experimentally investigating *task readiness impedance* in virtual tennis.

The virtual trajectory $X^*_{ey}(t)$ can be regarded as invariable in the preparation phase, so the task readiness impedance parameters in (15), M_e, B_e, and K_e can be estimated. Some aspects of human impedance mechanisms, such as functions of regulation and adaptation according to circumstances, can be exploited in terms of task readiness impedance, although task readiness impedance differs from human impedance in dynamic motion.

4.2 Accuracy of estimated impedance

Figure 13 illustrates the results of the accuracy testing of estimated impedance parameters in the developed virtual tennis system. A weight was attached to the racket handle of the robot while a spring was set between the handle and the environment. The intersections of the dotted lines in the figure represent the true values of the attached impedance to the robot handle. Note that both stiffness and inertia were estimated correctly, and the standard deviations for the stiffness and the inertia are less than 4.53 N/m and 0.01 kg, respectively.

4.3 Experiments

Task readiness impedance was investigated on four well-trained subjects who had received skill-acquisition training in virtual tennis and showed high success rates. To
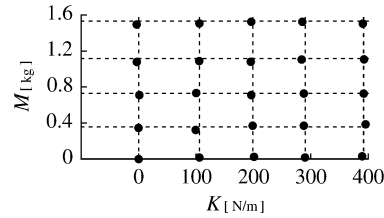
Fig. 13. Accuracy of estimated impedance parameters in the developed virtual tennis system, where the developed system was attached to already known spring-mass systems. A known weight was attached to the racket handle of the robot while a known spring was set between the handle and the environment. The intersections of the *dotted lines* in the figure represent the true values of the spring-mass system. Mean values for five sets of the estimated results are plotted. Note that both stiffness and inertia were estimated accurately, where the values of SD for the stiffness and the inertia are less than 4.53 N/m and 0.01 kg, respectively

change the impact force between the racket and the ball, two different ball masses, $M_b = 0.1, 0.5$ kg, were used, and two different handle viscosities were prepared to change the dynamic properties of the racket handle (K_r, B_r, M_r) = (0.0, 5.0, 1.0), (0.0, 20.0, 1.0) N/m, Ns/m, kg. The experiments were carried out under the following four conditions:

$$\text{I. } M_b = 0.1 \text{ kg}, B_r = 5.0 \text{ Ns/m} \qquad (16)$$
$$\text{II. } M_b = 0.5 \text{ kg}, B_r = 5.0 \text{ Ns/m} \qquad (17)$$
$$\text{III. } M_b = 0.1 \text{ kg}, B_r = 20.0 \text{ Ns/m} \qquad (18)$$
$$\text{IV. } M_b = 0.5 \text{ kg}, B_r = 20.0 \text{ Ns/m} \qquad (19)$$

Hand impedance along the y-axis was estimated by applying a disturbance at two different timings. The first disturbance was added at 2.5 s before the ball was thrown (before motion), and the second was at 0.7 s before the subject started moving the handle (task readiness). Table 2 shows the onset time of the disturbances in each condition for all subjects. The hand impedance was then estimated with 300 data points from the beginning of the onset time of the disturbance, assuming the virtual trajectory was constant. Figure 14 shows an example of the measured signals for impedance measurements, where the time histories of hand position $X_{ey}(t)$, hand velocity $\dot{X}_{ey}(t)$, hand acceleration $\ddot{X}_{ey}(t)$, and hand force $F_e(t)$ are given in order from left to right. The hand impedance parameters, K_e, B_e, and M_e, were estimated by using (15) with these time series.

Table 2. Onset time of disturbance for impedance measurements. The hand impedance was then estimated with 300 data points from the beginning of the onset time of the disturbance, assuming the virtual trajectory was constant

|	Experimental conditions			
Subjects	I (s)	II (s)	III (s)	IV (s)
A	2.60	2.65	2.65	2.75
B	2.65	2.65	2.75	2.65
C	2.65	2.60	2.65	2.65
D	2.60	2.65	2.75	2.60
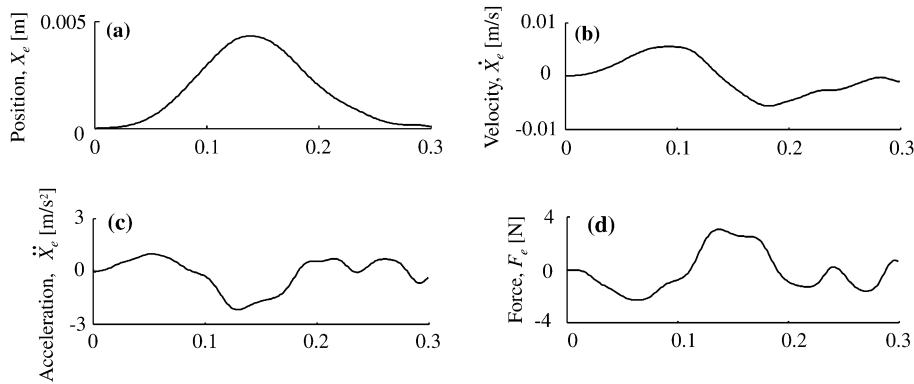
Fig. 14. Example of measured signals for measurement of task readiness impedance (subject A). Time histories of the hand position $X_{ey}(t)$, hand velocity $\dot{X}_{ey}(t)$, hand acceleration $\ddot{X}_{ey}(t)$, and hand force $F_e(t)$ are given in order from *left* to *right*

4.4 Analysis of human impedance

We first analyzed how the well-trained subjects adjusted their motions according to the experimental conditions. Figure 15 gives the mean values and the standard deviations of the hand motion at the moment of impact with the ball.

The subjects increased their hand force for hitting the large mass of the ball to counteract the interaction force (II and IV). It is difficult for a player to move a hand with rapid acceleration under highly viscous conditions (III and IV). Thus, the subjects took a larger backswing of the racket in order to hit the ball with sufficient velocity than when under less viscous conditions. This suggests that the well-trained subjects could adapt their dynamic motion according to circumstances.

Table 3 gives the mean values and standard deviations of the estimated impedance parameters for each task condition. Also, Figs. 16 and 17 show the changes of the hand stiffness and viscosity, respectively, depending on the task conditions.
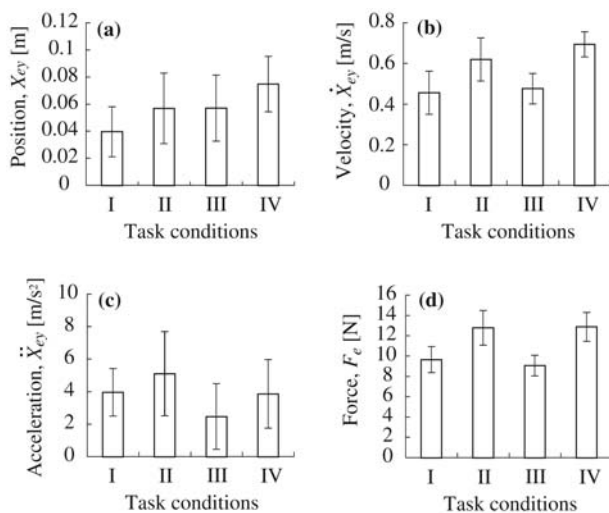
Fig. 15a–d. Hand motion at time of impact (subject A). The subjects increased their hand force to counteract the interaction force upon hitting the balls, where the mass of the ball was substantial (II and IV). Players move their hands with rapid acceleration under highly viscous conditions (III and IV)

Figure 16 and Table 3 indicate that the subjects increased their hand stiffness to prepare for impact under all experimental conditions. Note that the subjects stiffen their arms to respond to the impact force depending on the weight of the ball.

Moreover, comparing the experimental results of four subjects with different viscous environments under the same weight of the ball (I and III, II and IV), it can be seen from Fig. 17 that the hand viscosity of subjects A, B, and C in a less viscous environment becomes greater than in a more viscous environment. This suggests that a well-trained subject increases hand viscosity to maintain stability under a less viscous environment.

By contrast, subject D's hand viscosity increases in a more viscous environment than in a less viscous environment. Although subject D was regarded as a well-trained subject based on the rate of successful trials, he was the only player who increased his hand viscosity unnecessarily in more viscous environments. From the impedance point of view, subject D is a less skilled player compared to other well-trained players and needs to polish his skills. Impedance analysis in human movements reveals such subtle differences between players, differences that cannot be found through analysis of success rates.

5 Conclusion

This paper developed a virtual tennis system using an impedance-controlled robot as a first step toward realizing impedance training in dynamic motion. The process of acquiring skills was demonstrated through the analysis of dynamic characteristics of human arm movements in the training experiments with the measured EMG signals and arm postures. The task readiness impedance of the well-trained subjects was then investigated, and the following primary characteristics were clarified:

1. Subjects prepare for a motion by increasing hand stiffness.
2. Subjects change their hand stiffness according to the mass of the ball to control the interaction force.
3. Skilled subjects increase their hand viscosity in less viscous environments to maintain stability.

We can thus conclude that humans skillfully regulate hand impedance according to given tasks. The characteristics of

Table 3. Measured hand impedance during virtual tennis (subjects A–D). Mean values and SDs for five sets of estimated impedance parameters for each task condition

(a) Subject A

(i) Task condition I

	K_e [N/m]	B_e [Ns/m]	M_e [kg]	ρ
During maintenance of the stable posture	110.3±63.4	25.8±1.3	1.6±0.1	0.97±0.01
Before motion	125.0±40.0	26.4±1.4	1.6±0.1	0.97±0.01
Task readiness	124.1±59.0	26.4±0.9	1.5±0.1	0.97±0.01

(ii) Task condition II

	K_e [N/m]	B_e [Ns/m]	M_e [kg]	ρ
During maintenance of the stable posture	110.2±63.4	25.8±1.9	1.6±0.1	0.97±0.01
Before motion	128.1±34.3	26.2±1.8	1.6±0.1	0.97±0.01
Task readiness	147.3±47.3	26.3±1.1	1.6±0.1	0.97±0.01

(iii) Task condition III

	K_e [N/m]	B_e [Ns/m]	M_e [kg]	ρ
During maintenance of the stable posture	134.9±43.0	22.4±1.1	1.9±0.1	0.99±0.01
Before motion	151.1±42.3	22.5±1.2	1.8±0.1	0.97±0.01
Task readiness	164.9±78.0	22.8±3.5	1.9±0.2	0.97±0.02

(iv) Task condition IV

	K_e [N/m]	B_e [Ns/m]	M_e [kg]	ρ
During maintenance of the stable posture	134.9±43.0	22.4±1.1	1.9±0.1	0.99±0.01
Before motion	164.3±33.2	22.5±2.4	1.8±0.1	0.95±0.01
Task readiness	199.1±76.0	23.6±2.9	1.8±0.1	0.95±0.01

(c) Subject C

(i) Task condition I

	K_e [N/m]	B_e [Ns/m]	M_e [kg]	ρ
During maintenance of the stable posture	75.2±33.0	15.6±1.3	1.7±0.1	0.97±0.02
Before motion	81.3±43.2	17.1±1.4	1.8±0.1	0.97±0.01
Task readiness	110.8±17.9	17.6±2.7	1.8±0.1	0.97±0.01

(ii) Task condition II

	K_e [N/m]	B_e [Ns/m]	M_e [kg]	ρ
During maintenance of the stable posture	75.2±33.0	15.6±1.3	1.7±0.1	0.97±0.02
Before motion	89.1±43.2	15.6±1.9	1.6±0.1	0.97±0.01
Task readiness	158.0±34.7	17.1±1.1	1.7±0.1	0.97±0.01

(iii) Task condition III

	K_e [N/m]	B_e [Ns/m]	M_e [kg]	ρ
During maintenance of the stable posture	101.3±46.3	15.1±1.7	1.4±0.1	0.97±0.01
Before motion	103.7±49.1	15.3±1.2	1.3±0.1	0.97±0.01
Task readiness	127.9±56.1	15.4±1.7	1.3±0.1	0.97±0.01

(iv) Task condition IV

	K_e [N/m]	B_e [Ns/m]	M_e [kg]	ρ
During maintenance of the stable posture	101.3±46.3	15.1±1.7	1.4±0.1	0.97±0.01
Before motion	107.4±52.0	15.5±2.3	1.6±0.1	0.97±0.02
Task readiness	133.4±53.8	16.1±2.1	1.6±0.1	0.97±0.02

(b) Subject B

(i) Task condition I

	K_e [N/m]	B_e [Ns/m]	M_e [kg]	ρ
During maintenance of the stable posture	125.2±35.4	22.3±1.3	2.1±0.1	0.98±0.01
Before motion	126.0±44.2	22.6±1.1	2.2±0.1	0.98±0.02
Task readiness	126.1±30.6	22.7±1.0	2.2±0.1	0.98±0.02

(ii) Task condition II

	K_e [N/m]	B_e [Ns/m]	M_e [kg]	ρ
During maintenance of the stable posture	125.2±22.3	21.1±1.8	1.8±0.1	0.98±0.01
Before motion	145.3±63.1	23.8±3.6	1.8±0.2	0.98±0.02
Task readiness	175.9±59.2	26.2±3.3	1.8±0.2	0.98±0.02

(iii) Task condition III

	K_e [N/m]	B_e [Ns/m]	M_e [kg]	ρ
During maintenance of the stable posture	159.6±59.0	19.7±3.2	2.1±0.1	0.98±0.01
Before motion	179.8±57.6	19.7±1.7	2.2±0.1	0.97±0.02
Task readiness	190.9±49.4	22.1±3.2	2.2±0.1	0.97±0.02

(iv) Task condition IV

	K_e [N/m]	B_e [Ns/m]	M_e [kg]	ρ
During maintenance of the stable posture	159.6±59.0	19.7±3.2	2.1±0.1	0.98±0.01
Before motion	198.3±61.8	22.5±3.0	2.3±0.1	0.97±0.02
Task readiness	264.2±45.0	22.9±2.0	2.5±0.1	0.96±0.02

(d) Subject D

(i) Task condition I

	K_e [N/m]	B_e [Ns/m]	M_e [kg]	ρ
During maintenance of the stable posture	111.1±26.1	17.3±1.1	1.9±0.1	0.98±0.01
Before motion	114.3±48.6	17.7±2.3	1.8±0.1	0.97±0.01
Task readiness	125.8±30.3	18.7±1.3	1.9±0.0	0.98±0.01

(ii) Task condition II

	K_e [N/m]	B_e [Ns/m]	M_e [kg]	ρ
During maintenance of the stable posture	111.1±26.1	17.3±1.1	1.9±0.1	0.98±0.01
Before motion	119.1±32.0	17.4±2.2	2.0±0.1	0.98±0.01
Task readiness	138.0±39.1	17.7±1.0	2.0±0.0	0.98±0.01

(iii) Task condition III

	K_e [N/m]	B_e [Ns/m]	M_e [kg]	ρ
During maintenance of the stable posture	111.4±49.6	21.1±1.8	1.8±0.1	0.98±0.01
Before motion	134.9±72.7	21.6±2.3	1.8±0.1	0.97±0.01
Task readiness	172.3±50.6	23.2±3.1	1.8±0.2	0.97±0.01

(iv) Task condition IV

	K_e [N/m]	B_e [Ns/m]	M_e [kg]	ρ
During maintenance of the stable posture	111.4±49.6	21.1±1.8	1.8±0.1	0.98±0.01
Before motion	145.3±63.1	23.8±3.6	1.8±0.2	0.96±0.02
Task readiness	175.9±59.2	26.2±3.3	1.8±0.2	0.95±0.02

human hand impedance regulation have been reported. Mussa-Ivaldi et al. (1985) showed that humans cannot regulate the direction of hand stiffness. Tsuji et al. (1994, 1995) found that humans could regulate hand viscosity to some extent. Also, Tsuji et al. (1995) and Tsuji and Kaneko (1996) revealed that the magnitude of hand viscosity can be changed according to hand force. Gomi and Kawato (1997) demonstrated that humans regulate hand stiffness magnitude to be smaller in motion than in a stable posture. Although hand impedance characteristics have been analyzed in simple movements only, this research may have pioneered hand impedance measurements in task-related movements. The experimental results showed for the first time that humans can regulate hand stiffness and viscosity according to a given task. Note that the obtained results might be different if based on dynamic properties during real tennis. If in the future an experimental system capable of measuring three-dimensional forces and movements is constructed using the proposed method, the trainees may carry out an impedance regulation training that is similar to one used in real tennis.
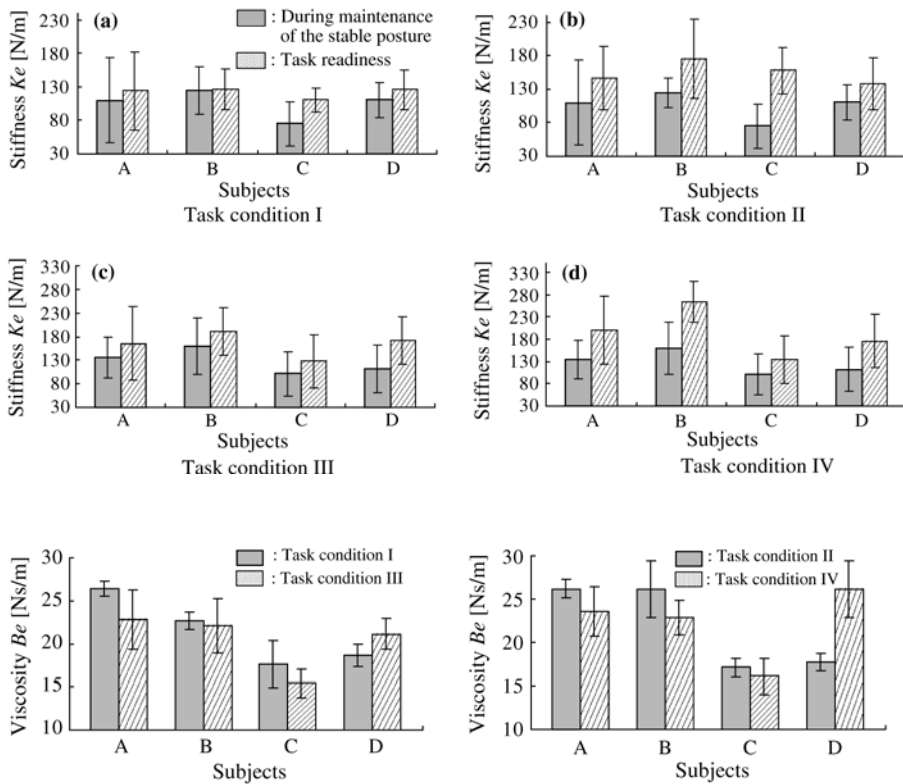
Fig. 16a–d. Hand stiffness during maintenance of stable posture and at task readiness. The subjects increased their hand stiffness to prepare for movements under all experimental conditions (I–IV)

(a) Comparison between task conditions I and III

(b) Comparison between task conditions II and IV

Fig. 17a–b. Hand viscosity at task readiness. Comparing the experimental results of subjects A–C with different viscous environments under the same ball weight (I and III, II and IV), it can be found that the hand viscosity in a less viscous environment becomes greater than in a more viscous environment. By contrast, the hand viscosity of subject D in a more viscous environment becomes greater than in a less viscous environment

Future research will be directed at measuring and analyzing hand impedance in two-dimensional movements. We also intend to collect task-related impedance data of human movements for application to sports training and rehabilitation. In that case, the dynamic systems theory needs to be combined with the proposed method to meticulously analyze complex movements such as cyclical movements in various sports Kurz and Stergiou (2004).

References

Dolan JM, Friendman MB, Nagarka ML (1993) Dynamics and loaded impedance of human arm posture. IEEE Trans Syst Man Cybern 23(3):698–709

Gomi H, Kawato M (1996) Equilibrium-point control hypothesis examined by measured arm stiffness during multijoint movement. Science 272:117–120

Gomi H, Kawato M (1997) Human arm stiffness and equilibrium-point trajectory during multi-joint movement. Biol Cybern 76:163–171

Hogan N (1985) Impedance control: an approach to manipulation, parts I, II, III. ASME J Dyn Syst Measure Control 107(1):1–24

Hogan N, Krebs HI, Charnnarong J, Srikrishna P, Sharon A (1993) MIT–MANUS: a workstation for manual therapy and training II. In: Proceedings of the conference on telemanipulator technology, 1833:28–34

Kawazoe Y (1992) CAE of tennis rackets with impact phenomena. Trans Jpn Soc Mech Eng 58(552):2467–2474 (in Japanese)

Krebs HI, Hogan N, Asen ML, Volpe BT (1996) Application of robotics and automation technology in neuro-rehabilitation. In: Proceedings of the US symposium on flexible automation 1:269–275

Kurz MJ, Stergiou N (2004) Applied dynamic systems theory for the analysis movement. In: Stergiou N (ed) Innovative analyses of human movement. Human Kinetics, Champaign, IL, pp 93–119

Mussa-Ivaldi FA, Hogan N, Bizzi E (1985) Neural, mechanical and geometric factors subserving arm in humans. J Neurosci 5(10):2732–2743

Osu R, Gomi H (1999) Multijoint muscle regulation mechanisms examined by measured human arm stiffness and EMG signals. J Neurophysiol 81(4):1458–1468

Tsuji T, Kaneko M (1996) Estimation and modeling of human hand impedance during isometric muscle contraction. Proc ASME Dyn Syst Control Div DSC 58:575–582

Tsuji T, Goto K, Ito K, Nagamachi M (1994) Estimation of human hand impedance during maintenance of posture. Trans Soc Instrum Control Eng 30(3):319–328(in Japanese)

Tsuji T, Morasso PG, Goto K, Ito K (1995) Human hand impedance characteristics during maintained posture. Biol Cybern 72:457–485

Tsuji T, Moritani M, Kaneko M, Ito K (1996) An analysis of human hand impedance characteristics during isometric muscle contractions. Trans Soc Instrum Control Eng 32(2):271–289 (in Japanese)

Tsuji T, Kanji H, Kato T, Kaneko M, Kawamura S (1999) Impedance training: can we regulate our hand impedance through training? Trans Soc Instrum Control Eng 35(10):1300–1306 (in Japanese)

Tsuji T, Sumida Y, Kaneko M, Kawamura S (2001) A virtual sports system for skill training. J Robot Mechatron 13(2):168–175